Electrochemistry Communications 182 (2026) 108087

Contents lists available at ScienceDirect

Electrochemistry Communications

journal homepage: www.elsevier.com/locate/elecom

Uniform secondary current distribution at disk electrodes under Tafel kinetics enabled by concentric current-shielding rings

Vaishnavi Sree Jeganathan, Rohan Akolkar *

Department of Chemical Engineering, Case Western Reserve University, Cleveland, OH 44106, USA

ARTICLE INFO

Keywords:
Rotating ring-disk electrode
Current distribution
Wagner number

ABSTRACT

Non-uniform secondary current distribution at rotating disk electrodes (RDE) is a common problem when using resistive electrolyte media or large applied currents. In a recent publication, we have shown that auxiliary electrodes such as the ring of a rotating ring-disk electrode (RRDE) can help suppress current non-uniformities at the disk enabling reliable electroanalytical measurements. However, this previous work considered linear kinetics where current distribution non-uniformities were moderate. In the present contribution, we consider current distribution non-uniformities encountered under Tafel kinetics. We show, for the case of 2,5-dihydroxy-1,4-benzoquinone (DHBQ) reduction, that optimally chosen ring conditions serve to provide effective shielding at the disk edge rendering the overall disk current distribution to be uniform. Numerical modeling and scaling analysis (using the Wagner number) are presented to aid a user in determining the optimal ring current density for achieving uniform disk current distribution under Tafel kinetics. This approach is especially useful when studying soluble-soluble redox transitions for which, unlike deposit distribution in electrodeposition, the current distribution non-uniformity is not visually apparent.

1. Introduction

Rotating disk electrodes (RDE) are commonly employed in electroanalytical studies. However, when operated in regimes where mass-transport (i.e., diffusional) limitations are negligible, these electrodes can suffer from a non-uniform 'secondary' current distribution, i.e., the current is concentrated more towards the disk edges than near its center. This non-uniformity can have many negative ramifications: erroneous electrode kinetics measurements, distortions in transient voltammetric data, wrong inferences about electrocatalytic effects, misrepresentation of reaction performance parameters such as efficiencies or selectivities, and non-uniform deposit distribution (for electrodeposition). Non-uniformity of the current is more pronounced in systems with low ionic conductivity or when high average current densities are applied. The secondary current distribution non-uniformity is characterized by a dimensionless parameter called the Wagner number (Wa), which is defined as the ratio of the activation resistance (R_A, associated with charge-transfer) to the ohmic resistance (R_Ω, associated with migrational transport through the electrolyte). For a disk electrode of radius r_0, and assuming Tafel kinetics, Wa is [1]:

$$\mathrm{Wa} = \frac{R_A}{R_\Omega} = \frac{4\kappa RT}{\pi F\alpha i_{avg} r_0} \tag{1}$$

Low Wa values indicate dominance of ohmic resistance, leading to a highly non-uniform current distribution. Electrolytes in which ohmic resistance is typically large are viscous media like deep eutectic solvents, water-in-salt electrolytes, and ionic liquids [2]. To address current density 'hot spots' at the disk edge due to secondary current distribution, auxiliary electrodes commonly known as 'shielding' or 'thief' electrodes are employed. In a recent paper by Jeganathan et al. [3], a ring-disk electrode (RRDE) was employed whereby the ring, when polarized optimally, served to shield the disk from high current density regions thereby uniformizing current distribution. Numerical modeling and scaling analysis were then used to identify the optimal ring conditions, e.g., the ring potential or current, for the case of $Cu^{2+} + e = Cu^{1+}$ redox reaction in a deep eutectic solvent under linearized kinetics ($|\eta_a| < 20$ mV). The approach followed by Jeganathan et al. bears similarities with that proposed much earlier by Mehdizadeh et al. [4], who employed a concentric ring 'thief' electrode to modulate the current distribution during Cu deposition on a large diameter silicon wafer. It must be noted that the idea of current shielding (one electrode shielding current when placed in the vicinity of another) is widely practiced in electroanalytical

* Corresponding author.
E-mail address: rna3@case.edu (R. Akolkar).

https://doi.org/10.1016/j.elecom.2025.108087
Received 26 May 2025; Received in revised form 18 June 2025; Accepted 24 November 2025
Available online 24 November 2025
1388-2481/© 2025 The Authors. Published by Elsevier B.V. This is an open access article under the CC BY-NC license (http://creativecommons.org/licenses/by-nc/4.0/).

measurements [5–7]; however, prior works commonly address mass-transport limited regimes in which the ring and disk operate in a generator-collector arrangement. Prior studies largely ignore the case of secondary current distribution whereby the ring and disk influence the potential fields in their vicinity and thus modulate the secondary current distribution.

This study extends the approach of Jeganathan et al. [3] to include Tafel kinetics representative of many practical electrochemical systems operating at high current densities or overpotentials. As a model reaction, we consider the electrochemical reduction of 2,5 Dihydroxy 1,4 Benzoquinone (DHBQ) in an aqueous electrolyte. This model system is relevant to redox flow-batteries [8], and allows us to operate at high current densities (>0.1 A/cm^2) without experiencing mass transport limitations, and ensuring Tafel kinetics behavior. Here, we first investigate the effects of current distribution on the steady-state polarization behavior of this system on a RDE. We then investigate how the outer concentric ring electrode of a RRDE aids in rectifying the current distribution at the inner disk electrode. Guidelines for choosing the optimal ring parameters are developed and correlated to the Wagner number (Eq. (1)). Our approach is beneficial when studying soluble-soluble redox transitions where, unlike in electrodeposition, the current non-uniformity is not visually apparent. It is also generalizable and is not limited to the particular redox system or electrode materials used in this study.

2. Experiments

2.1. Electrochemical cell setup

Electrolytes contained 2,5 Dihydroxy 1,4 Benzoquinone (DHBQ, 98 %, Thermo Scientific) at a concentration of 375 mM in a 1 M aqueous potassium hydroxide solution (KOH, Sigma Aldrich). The electrolyte was stirred at 40 °C for 1 h until DHBQ dissolved completely. Colour of the electrolyte was deep crimson red. Rotating ring-disk electrode (RRDE) with glassy carbon disk and Pt ring (Part no: AFE8R4GCPT, mirror polished, Pine Research Instrumentation Inc.) with disk radius of 0.25 cm, inner ring radius of 0.3 cm and outer ring radius of 0.425 cm was used. Experiments were carried out using separate potentiostats for the parallel ring and the disk circuits with care taken to avoid interferences. A Princeton Applied Research PARSTAT-4000 potentiostat was connected to the ring circuit, and a Princeton Applied Research VERSASTAT4–400 potentiostat was connected to the disk circuit. Reference electrodes and counter electrodes were separate for the disk and the ring circuits. A Pt wire was used as counter electrode. Commercially available Ag/AgCl (4 M KCl) electrodes served as reference electrodes.

2.2. Polarization experiments

Steady-state polarization experiments were carried out at 23 ± 2 °C. RRDE rotation was maintained at 2500 RPM in all experiments, which ensured minimal mass transport limitations. Solution resistance at the disk in the absence of any ring current ($R_{\Omega-\mathrm{d}}$) was measured using electrochemical impedance spectroscopy (EIS). In experiments, the activation overpotential (η_a) corresponding to DHBQ reduction was obtained from:

$$\eta_\mathrm{a} = V_\mathrm{app} - E_\mathrm{eq} - \eta_\mathrm{c} - \left(I_\mathrm{d}R_{\Omega-\mathrm{d}} + I_\mathrm{ring}R_{\Omega-\mathrm{dr}}\right) \tag{2}$$

Here, V_app is the applied potential, E_eq is the equilibrium potential, and η_c is the concentration overpotential. $R_{\Omega-\mathrm{d}}$ obtained from EIS was 20.8 Ω. $R_{\Omega-\mathrm{dr}}$, i.e., the disk resistance in the presence of the ring current, was measured following the potential-step protocol described earlier [3]. Briefly, a fixed current (20 mA cm^{-2}) was applied to the disk while no net current was applied to the ring. Following this, a current step was applied to the ring and the change in the disk potential was recorded. The potential change at the disk due to the presence of various ring currents was plotted and this yielded the value of $R_{\Omega-\mathrm{dr}}$ (=8.68 Ω).

3. Results and discussion

3.1. Effects of non-uniform secondary current distribution on polarization

Under non-uniform current distribution, the high local current densities at the disk edges lead to a shift in the effective polarization curve (i_avg vs. η_a) towards higher magnitudes of η_a [3]. Conversely, irregularities in the polarization behavior can be a symptom of non-uniformity in the secondary current distribution. To quantify the influence of current distribution non-uniformity on Tafel polarization, we performed numerical simulations of secondary current distribution by solving Laplace's equation:

$$\nabla^2\phi = 0 \tag{3}$$

At the disk and the ring boundaries, Tafel kinetics prevail:

$$\text{disk}: \nabla\phi = -\frac{i_0}{\kappa}e^{-\alpha f(V_\mathrm{d}-\phi)} \tag{4}$$

$$\text{ring}: \nabla\phi = -\frac{i_0}{\kappa}e^{-\alpha f(V_\mathrm{r}-\phi)} \tag{5}$$

$f = F/RT$ where F is Faraday's constant, R is the ideal gas constant, and T is temperature. i_0 is the exchange current density and α is the charge transfer coefficient for DHBQ reduction, κ is the electrolyte conductivity, and V_d and V_r are the applied potentials at the disk and the ring, respectively. At all insulating boundaries, a no flux condition ($\nabla\phi = 0$) was applied. At the counter electrode placed far away from the disk, the potential V_CE was set to zero. In the absence of the ring current, the activation overpotential at the disk was calculated using:

$$\eta_\mathrm{a} = V_\mathrm{d} - V_\mathrm{CE} - I_\mathrm{d}R_{\Omega-\mathrm{d}} \tag{6}$$

where $R_{\Omega-\mathrm{d}} = (4\kappa r_0)^{-1}$ is the disk ohmic resistance [9]. Fig. 1 presents the simulated Tafel curve (i_avg vs. η_a) on a disk electrode. As noted, with increasing η_a, the Wagner number (Wa) decreases as a result of increased i_avg. The simulated Tafel curve (red) is closer to the ideal Tafel slope (dashed) at relatively higher Wa as expected, but it shows a marked deviation from ideality as Wa decreases. As Wa approaches values close to 0.1, deviations become prominent leading to a significantly different Tafel slope ($\alpha = 0.39$). Deviation in the Tafel slope from the ideal line (dashed) is due to the effects of the non-uniformity in current distribution. Such non-uniformity also results in a non-uniform ohmic drop across the disk surface, making the use of a single value of $R_{\Omega-\mathrm{d}}$ (Eq. (6)) inaccurate [9,10].

3.2. Correction of the polarization curve accounting for current distribution

Fig. 2a presents experimental polarization data (blue) in the Tafel regime for DHBQ reduction on a disk electrode at 2500 RPM. First, no signs of mass-transport limitations were observed, i.e., small η_c. Second, in experimental data too, non-linearity in the Tafel curve is observed especially at overpotentials negative with respect to −0.207 V ($i_\mathrm{avg} = -58$ mA cm^{-2}, Wa = 0.21), suggesting that this deviation in Tafel slope is due to the effect of non-uniform secondary current distribution. This was further confirmed by numerical simulations (red) which capture the non-linearity in the Tafel slope. The steady state model fits the experimental data well, within an error of <5 mV. Thus, it is reasonable to assume that transient effects due to adsorption and double-layer charging are minimal. Here, simulations (Eqs. (3), (4), (6)) were performed assuming $\alpha = 0.5$ and $i_0 = 1.2$ mA cm^{-2}, but they yielded an i_avg corresponding to a much lower 'effective' α similar to experiments (Fig. 1).

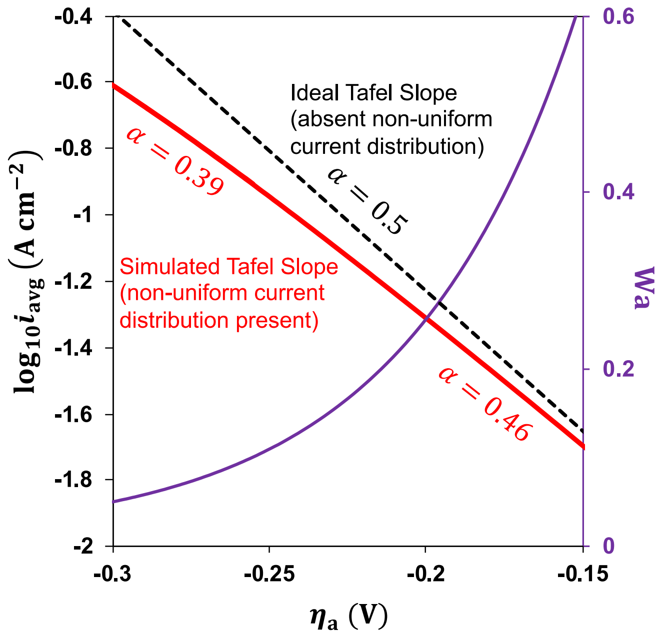

Fig. 1. Simulated polarization curve (red) on a disk electrode (assuming no ring is present) using model described by Eq. 3–6 for $\alpha = 0.5$, $i_0 = 1.2$ mA cm^{-2}, and $\kappa = 48.1$ mS cm^{-1}. Primary Y-axis shows average current density (i_{avg}) obtained via a surface integral of the current density profile over the disk. Secondary axis (purple) shows the computed Wa number (Eq. 1), which depends on i_{avg}. As Wa decreases, the computed Tafel slope deviates from ideality due to non-uniform current distribution such that the 'effective' value of α is lower compared to its true value (=0.5). (For interpretation of the references to colour in this figure legend, the reader is referred to the web version of this article.)

A strategy to correct experimental polarization curves is to apply an ohmic resistance correction that accounts for the spatial non-uniformity of current distribution. Newman [9] and Esteban et al. [10] explain how such a modified ohmic correction can be performed by referencing to the current density and the corresponding activation overpotential at the center of the disk (i_{cntr}, η_{a-cntr}). Using a theoretically-derived correction factor (which itself depends on the extent of current distribution non-uniformity) given by Newman [9], i_{cntr} and η_{a-cntr} can be extracted from experimental polarization data. The correction factor (CF) ranges from 1 for primary distribution to 1.273 for uniform secondary distribution and can be used to compute η_{a-cntr} as:

$$\eta_{a-cntr} = V_{app} - E_{eq} - \eta_c - I_d R_{\Omega-d}(\mathrm{CF}) \tag{7}$$

Fig. 2b (green data points) shows the corrected experimental polarization curve plotting i_{cntr} vs. η_{a-cntr}. It is seen that the corrected polarization curve is in better agreement with the expected Tafel curve ($\alpha = 0.5$, dashed line). This establishes secondary current distribution and associated non-uniformities as the key factors causing deviation of experimental polarization data away from ideality. Appropriate corrections [9,10] to account for such factors eliminate irregularities and put data and theory ($\alpha = 0.5$) in good accord.

3.3. *Uniformizing disk current distribution using current-shielding ring*

Polarization measurements were performed for DHBQ reduction on an RRDE where the disk and the ring were held galvanostatically. The average disk current was -102 mA cm^{-2} and the average ring current was varied. RRDE rotation (2500 RPM) ensures that species generated at the ring are swept away from the disk due to the flow pattern at the RRDE. Here, the function of the ring is to divert current away from the disk edge, thereby uniformizing the disk current distribution [3]. The ratio of the average ring current density to the fixed disk current density, referred to as θ, was varied. The optimal value of θ, and thus the optimal ring current density, is that for which the disk current distribution is most uniform. This corresponds to the case where the activation overpotential (η_a, Eq. (2)) at the disk falls on the 'Ideal Tafel Slope' ($\alpha = 0.5$, dashed line) in Fig. 3. As Fig. 3 shows, the magnitude of the activation overpotential decreases as θ (or the ring current density) increases (black unfilled circles). At θ values in the range 3–5 (red unfilled circles), η_a is in close agreement with that expected for $\alpha = 0.5$, suggesting that applying a ring current density that is 3–5 times the disk current density provides the optimal condition to eliminate the current non-uniformity at the disk edge.

Fig. 4a and b present the current density profiles obtained from simulations (Eqs. (3)–(6)) at the disk and ring, respectively. Simulations were performed for a variety of ring currents represented by θ ranging from 0 to 6.5. As θ (and thus ring current density) increases, a significant

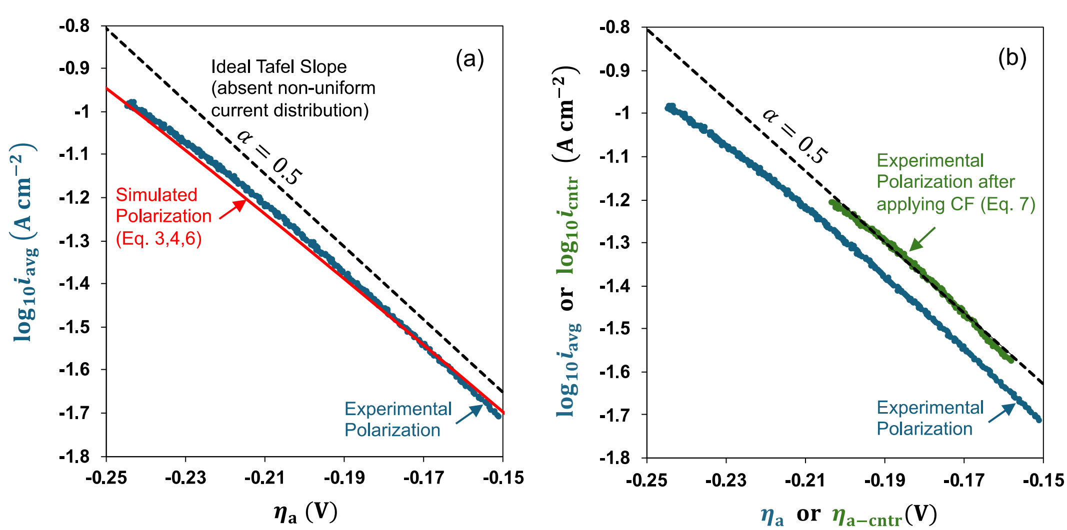

Fig. 2. (a) Experimental polarization (blue) for the reduction of 375 mM DHBQ in 1 M KOH on RDE shows non-linearity at more negative overpotentials, which is due to secondary current distribution non-uniformity. Current distribution simulations (red) capture the experimentally observed deviations from linearity. (b) Experimental polarization data corrected for secondary current distribution effects (using CF in Eq. (7) [9,10], green) to yield the center current density (i_{cntr}) and the center activation overpotential (η_{a-cntr}). After correction, data agrees with expected Tafel slope ($\alpha = 0.5$, dashed line). (For interpretation of the references to colour in this figure legend, the reader is referred to the web version of this article.)

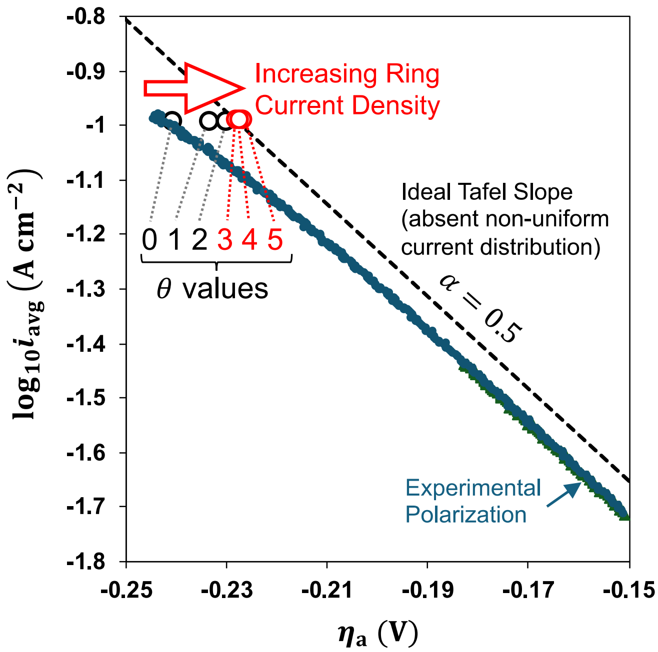

Fig. 3. Experimental RRDE data (2500 RPM) for DHBQ reduction in 1 M KOH. The disk current density was fixed at -102 mA cm^{-2} (black circles), and the average ring current density was varied. The factor θ, representing the ratio of ring-to-disk current densities, was varied from 0 to 5. The optimal range of θ to rectify current distribution non-uniformity leading to a close match with ideal kinetics ($\alpha = 0.5$) is 3–5.

drop (shielding) of the disk edge current density is seen together with noticeable uniformity of the disk current distribution. Fig. 4a indicates that the most uniform disk current density profile is observed when θ is between 4.45 and 4.75, generally consistent with the observed optimal θ range (3–5) in experiments (Fig. 3). Between θ values of 3 and 5 (inset), the standard deviation (σ) of the disk current density is within 10 % of its average, and σ increases if θ falls outside this optimal range. This is understood from the profiles in Fig. 4a, which show that, if $\theta > 6$, the disk current distribution profile exhibits an inversion, i.e., the disk edge current density falls below i_{avg} – this condition is also sub-optimal for applying the ring as an effective shield.

In the RRDE system, achieving uniform disk current distribution requires that the non-uniformity at the disk edge is isolated to the ring region [8]. This is comparable to the case in which the disk and ring are considered part of one larger disk such that the maximal current density at this larger disk becomes the applied ring current density of the RRDE. In our previous study, we provided an analytical expression for the ring-to-disk current density (θ) ratio based on Wa [3]:

$$\theta \approx \frac{\mathrm{Wa}^{-\frac{1}{2}}}{\tanh\left(\mathrm{Wa}^{-\frac{1}{2}}\right)} \tag{8}$$

At disk average current density $|i_{avg}| = 102$ mA cm^{-2}, the value of Wa is 0.073. This provides θ (via Eq. (8)) of 3.7, which is close to the optimal θ determined experimentally (Fig. 3) and numerically (Fig. 4). While Eq. (8) entails several simplifying assumptions [3], it can still be a good guide to users for choosing ring conditions for uniform disk current distribution.

4. Conclusions

An approach is presented for rectifying current distribution non-uniformity on a disk electrode. The approach involves employing a concentric ring 'shield' in a RRDE arrangement and applying high current density on the ring to divert current away from the disk edge thereby uniformizing the disk current distribution. This is demonstrated for the specific case of 2,5-dihydroxy-1,4-benzoquinone reduction in an aqueous medium, but the overall approach developed here is broadly applicable to other systems. Numerical modeling and scaling analysis (using Wa) are presented to aid a user in determining the ring current density for achieving uniform disk current distribution under Tafel kinetics. The findings presented herein are useful when the current distribution non-uniformity is not visually apparent and requires indirect probes for assessing and rectifying it.

CRediT authorship contribution statement

Vaishnavi Sree Jeganathan: Writing – original draft, Methodology, Investigation, Formal analysis, Conceptualization. **Rohan Akolkar:**

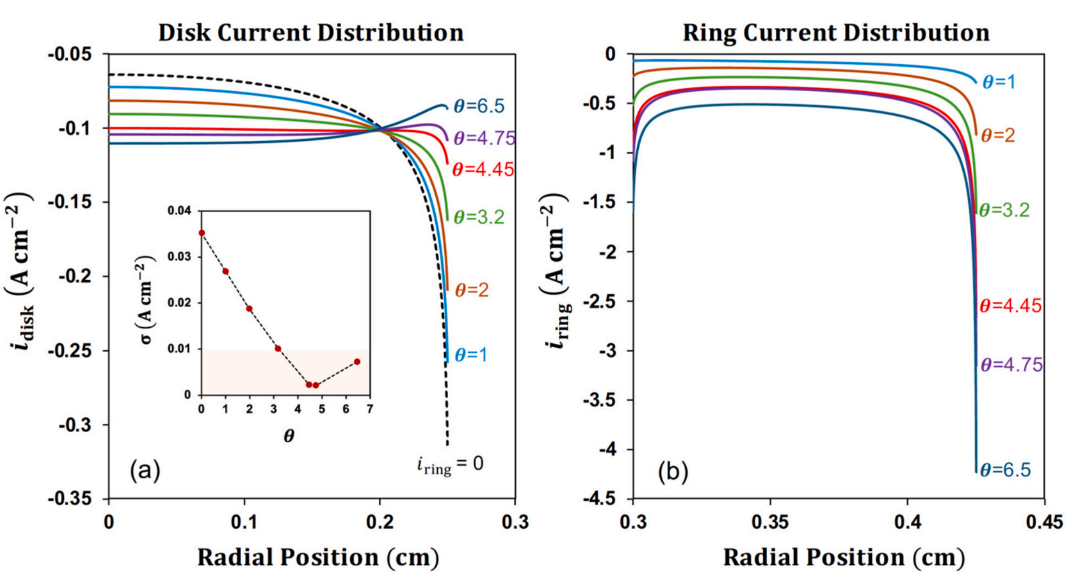

Fig. 4. (a) Simulated disk current density profiles (Eqs. (3)–(6)) for a range of ring current densities corresponding to $\theta = 1$, 2, 3.2, 4.45, 4.75, and 6.5. Inset shows standard deviation in current density with a minima near $\theta = 4.75$. Average disk current density was -102 mA cm^{-2} in all cases. (b) Ring current density profiles for all cases shown in (a).

Writing – review & editing, Supervision, Resources, Project administration, Investigation, Funding acquisition, Conceptualization.

Declaration of competing interest

The authors declare that they have no known competing financial interests or personal relationships that could have appeared to influence the work reported in this paper.

Acknowledgements

This work was supported by Breakthrough Electrolytes for Energy Storage – an Energy Frontier Research Center funded by the U.S. Department of Energy, Office of Science, Basic Energy Sciences, under Award #DE-SC0019409.

Data availability

Data will be made available on request.

References

[1] G.A. Prentice, Electrochemical Engineering Principles, Prentice Hall, 1990.
[2] R. Ghahremani, R.F. Savinell, B. Gurkan, J. Electrochem. Soc. 169 (2022) 030520.
[3] V.S. Jeganathan, N. Sinclair, R. Akolkar, ACS Electrochem. (2025), https://doi.org/10.1021/acselectrochem.4c00238.
[4] S. Mehdizadeh, J. Dukovic, P.C. Andricacos, L.T. Romankiw, H.Y. Cheh, J. Electrochem. Soc. 137 (1990) 110.
[5] W.J. Albery, M.L. Hitchman, Ring-Disc Electrodes, Clarendon Press, 1971.
[6] P.R. Unwin, R.G. Compton, J. Electroanal. Chem. Interfacial Electrochem. 274 (1) (1989) 249.
[7] G. Neubert, E. Gorman, R. Van Reet, K.B. Prater, J. Electrochem. Soc. 119 (6) (1972) 677.
[8] Z. Yang, L. Tong, D.P. Tabor, E.S. Beh, M.-A. Goulet, D. De Porcellinis, A. Aspuru-Guzik, R.G. Gordon, M.J. Aziz, Adv. Energy Mater. 8 (2018) 1702056.
[9] J. Newman, J. Electrochem. Soc. 113 (1966) 1235.
[10] J.M. Esteban, M. Lowry, M.E. Orazem, in: R. Taylor, L. Scribner (Eds.), The Measurement and Correction of Electrolyte Resistance in Electrochemical Tests, ASTM International, 1990.